An Ultra-Wideband CMOS Low Noise Amplifier for 3–5-GHz UWB System

Chang-Wan Kim, Min-Suk Kang, Phan Tuan Anh, Hoon-Tae Kim, and Sang-Gug Lee

***Abstract*—An ultra-wideband (UWB) CMOS low noise amplifier (LNA) topology that combines a narrowband LNA with a resistive shunt-feedback is proposed. The resistive shunt-feedback provides wideband input matching with small noise figure (NF) degradation by reducing the *Q*-factor of the narrowband LNA input and flattens the passband gain. The proposed UWB amplifier is implemented in 0.18-μm CMOS technology for a 3.1–5-GHz UWB system. Measurements show a −3-dB gain bandwidth of 2–4.6 GHz, a minimum NF of 2.3 dB, a power gain of 9.8 dB, better than −9 dB of input matching, and an input IP3 of −7 dBm, while consuming only 12.6 mW of power.**

***Index Terms*—Broadband, CMOS, feedback, low noise amplifier, RF, ultra-wideband.**

I. Introduction

RECENTLY, the interest in ultra-wideband (UWB) system for wireless personal area network (WPAN) application has increased significantly, though the international standard has yet to be finalized. The allocated frequency band of the UWB system is 3.1–10.6 GHz (low-frequency band: 3.1–5 GHz; high-frequency band: 6–10.6 GHz). Two recent major proposals [1], [2] for the IEEE 802.15.3a propose that data rates of up to 400–480 Mb/s can be obtained using only the low-frequency band. The low-frequency band has been allocated for the development of the first-generation UWB system. CMOS technology is a satisfactory choice for the implementation of the low band UWB system when considering the time to market, hardware cost, the degree of difficulty, etc.

Until now, reported CMOS-based wideband amplifiers tend to be dominated by two different topologies: the distributed and resistive shunt-feedback amplifiers. The distributed amplifiers [3], [4] normally provide wide bandwidth characteristics but tend to consume large dc current due to the distribution of multiple amplifying stages, which makes them unsuitable for low-power application. The resistive shunt-feedback-based amplifiers [5], [6] provide good wideband matching and flat gain, but tend to suffer from poor noise figure (NF) and large power dissipation. In the resistive shunt-feedback amplifier, input resistance is determined by the feedback resistance divided by the loop-gain of the feedback amplifier [7]. Therefore, the feedback resistor tends to be a few hundred ohms in order to match the low signal source resistance of typically 50 Ω, leading to significant NF degradation. Furthermore, even with a moderate amount of voltage gain, the amplifier requires a rather large amount of current, especially in the CMOS, due to its strong dependence for voltage gain on the transconductance of the amplifying transistor. Recently, a new topology of a wideband amplifier for UWB system, which adopts a bandpass LC filter at the input of the cascode low noise amplifier (LNA) for wideband input matching, has been reported in [8] and [9]. The bandpass filter-based topology incorporates the input impedance of the cascode amplifier as a part of the filter, and shows good performances while dissipating small amounts of dc power. However, the adoption of the LC filter at the input mandates a number of reactive elements, which could lead to a larger chip area and NF degradation in the case of on-chip implementation, or the additional external components.

This paper proposes a new low power, low noise, and wideband amplifier combining a narrowband LNA with the conventional resistive shunt-feedback. The design principles and the measurement results of the implemented 3.1–5-GHz UWB LNA are described.

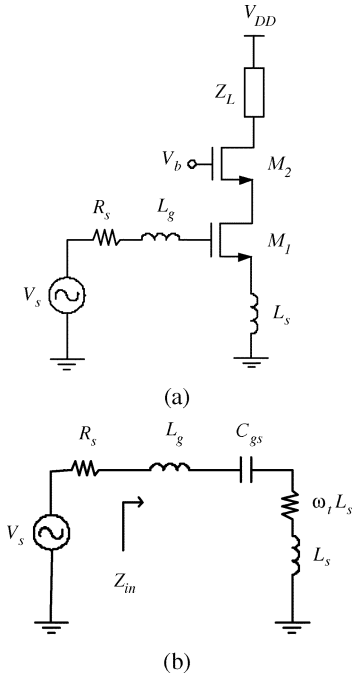

Fig. 1. Narrowband LNA topology. (a) Overall schematic. (b) Small-signal equivalent circuit at the input.

II. Design of Wideband Amplifier

Fig. 1(a) shows a typical narrowband cascode LNA topology. In Fig. 1(a), the inductor L_s is added for simultaneous noise and input matching and L_g for the impedance matching between the source resistance R_s and the input of the LNA [10]. Fig. 1(b) shows the small-signal equivalent circuit for the input part of the overall LNA, where C_{gs} represents the gate-source capacitance of the input transistor M_1. In Fig. 1(b), a series combination

Manuscript received April 8, 2004; revised August 26, 2004.

C.-W. Kim, M.-S. Kang, P. T. Anh, and S.-G. Lee are with the Information and Communications University, Yuseong, Daejeon, 305-600, Korea (e-mail: cwkim@icu.ac.kr).

H.-T. Kim is with the Samsung Advanced Institute of Technology, Suwon 440-600, Korea.

Digital Object Identifier 10.1109/JSSC.2004.840951

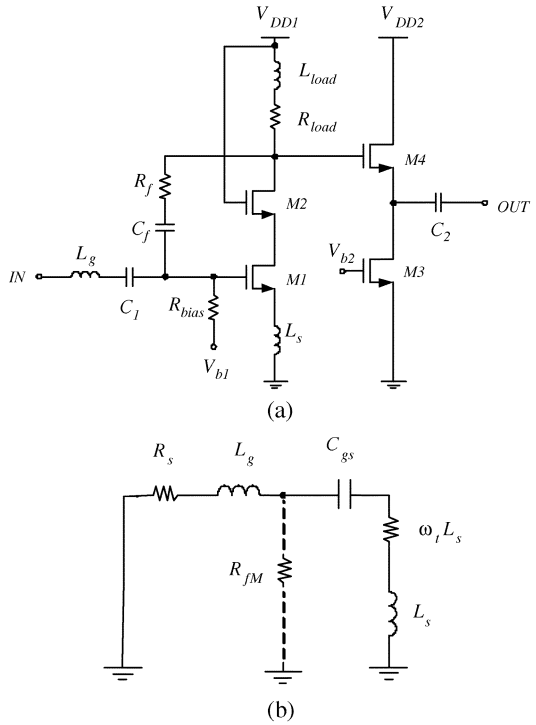

Fig. 2. UWB LNA topology. (a) Overall schematic. (b) Small-signal equivalent circuit at the input.

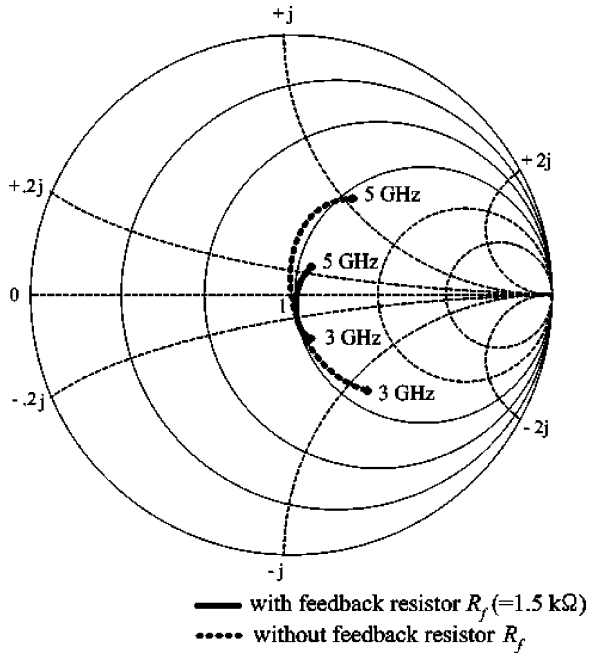

Fig. 3. Simulated S_{11} traces of LNA with or without the feedback resistor for frequencies over 3–5 GHz.

of reactive elements is chosen to resonate at the frequencies of interest such that Z_{in} becomes a real value with $\omega_T L_s$ being equal to R_s. The ω_T represents the cutoff frequency of transistor M_1. The quality factor Q of the series resonating input circuit shown in Fig. 1(b) can be given by [11]

$$Q_{NB} = \frac{1}{(R_S + \omega_T L_S) \cdot \omega_0 \cdot C_{gs}} \tag{1}$$

where ω_0 represents the resonant frequency. With a typical LNA, the Q-factor shown in (1) is generally preferred to be high for high-gain and low-noise performance while dissipating low dc power. Since the fractional -3-dB bandwidth of a typical RLC series resonant circuit is inversely proportional to its Q-factor ($\mathrm{BW}_{-3\mathrm{dB}} = \omega_0/Q_{NB}$), the LNA shown in Fig. 1(a) is unsuitable for wideband application.

Fig. 2(a) shows the proposed wideband LNA topology. In Fig. 2(a), R_f is added as a shunt-feedback element to the conventional cascode narrowband LNA and L_{load} is used as shunt peaking inductor at the output [12]. The capacitor C_f is used for the ac coupling purpose. The source follower, composed of M_3 and M_4, is added for measurement proposes only, and provides wideband output matching. C_1 and C_2 are ac coupling capacitors.

Fig. 2(b) shows the small-signal equivalent circuit for the input part of the proposed wideband LNA. In Fig. 2(b), the resistor $R_{fM}[= R_f/(1 - A_v)]$ represents the Miller equivalent input resistance of R_f, where A_v is the open-loop voltage gain of the LNA. From Fig. 2(a) and (b), the value of R_f can be much larger than that of the conventional resistive shunt-feedback. In the conventional resistive shunt-feedback, the size of R_f is limited as R_{fM} determines the input impedance. However, in the proposed topology, the input impedance is determined by $\omega_T L_s$. Therefore, in Fig. 2(a), one of the key roles of the feedback resistor R_f is to reduce the Q-factor of the resonating narrowband LNA input circuit. The Q-factor of the circuit shown in Fig. 2(b) can be approximately given by

$$Q_{WB} \approx \frac{1}{\left[R_S + \omega_t L_S + \frac{(\omega_0 L_g)^2}{R_{fM}}\right] \cdot \omega_0 \cdot C_{gs}}. \tag{2}$$

From (2), and considering the inversely linear relation between the -3-dB bandwidth and the Q-factor, the narrowband LNA in Fig. 2(a) can be converted into a wideband amplifier by the proper selection of R_f.

For example, to design a wideband amplifier that covers a certain frequency band, the narrowband amplifier will be optimized at the center frequency. Then, the -3-dB bandwidth of the small-signal equivalent input circuit can be set by the proper selection of R_f. Depending on the amount of bandwidth, the required value of R_f can vary and so will the amount of noise contribution by R_f. Fig. 3 shows the simulated S_{11} of the designed UWB amplifier with $R_f(= 1.5\,\mathrm{k}\Omega)$ and compares that of the amplifier without the feedback resistor R_f. As can be seen in Fig. 3, compared to the narrowband case, the addition of R_f gathers the values of passband S_{11} closer to the center of the Smith chart, leading to wideband input matching. The feedback resistor R_f also provides its conventional roles of flattening the gain over a wider bandwidth of frequencies with much smaller noise figure degradation.

III. Amplifier Design and Measurement Results

The proposed topology shown in Fig. 2(a) is applied to a 3.1–5-GHz wideband amplifier based on 0.18-μm CMOS technology. The narrowband LNA is optimized at 4 GHz by the

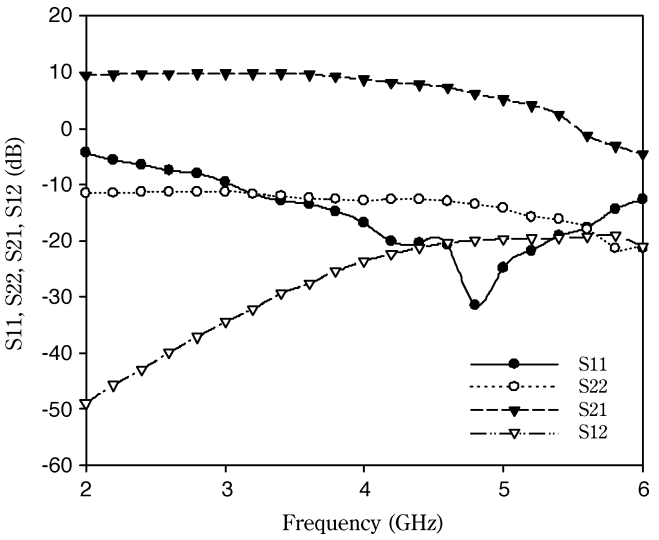

Fig. 4. Measured power gain, input/output return loss, and reverse isolation of the UWB LNA.

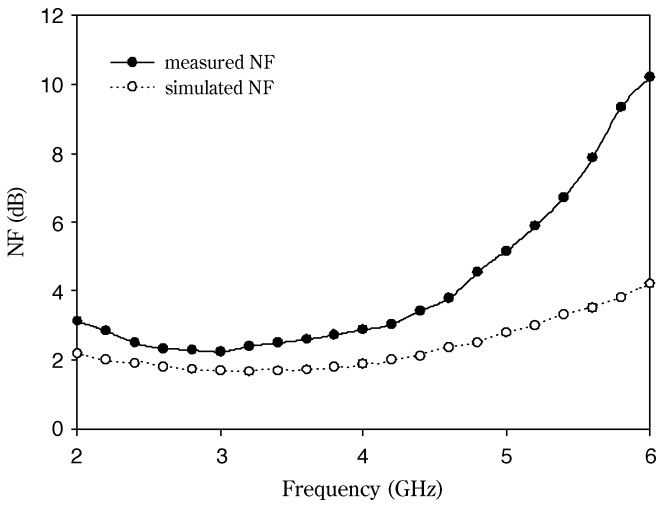

Fig. 5. Measured and simulated NF of the UWB LNA.

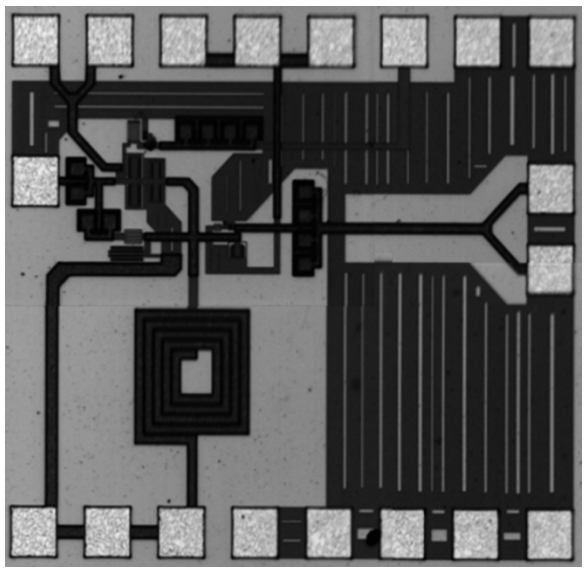

Fig. 6. Microphotograph of the fabricated UWB CMOS LNA. The inductors L_g and L_s are implemented as external components.

proper selection of the values for L_s and L_g. With feedback resistor R_f, the bandwidth extends to cover 3–5 GHz. In Fig. 2(a), the input transistor $M_1(W/L = 320/0.18\ \mu\text{m})$ is biased at 7 mA. The size of the cascode transistor $M_2(240/0.18\ \mu\text{m})$ is decided considering a trade-off between gain (S_{21}) and -3-dB bandwidth. The value of the on-chip spiral inductor L_{load} is 2.4 nH, and its quality factor (Q) is about 9.5 at 5 GHz. The source follower, which consists of $M_3(80/0.18\ \mu\text{m})$ and $M_4(40/0.35\ \mu\text{m})$, consumes 2 mA. Although $R_f = 1.5\ \text{k}\Omega$ is optimal from the simulation results due to the respectable noise performance, the value of R_f is adjusted as 1 kΩ in order to guarantee wideband input matching. In Fig. 2(a), the inductors L_s and L_g are implemented as external components with a value of 0.6 nH and 2.5 nH, respectively. These inductors can be absorbed as a part of the package parasitics, but in this work they are implemented with bond wires due to the chip-on-board (COB) evaluation of the fabricated chip. Other component values are $C_1 = C_f = 2$ pF, $C_2 = 4$ pF, and $R_{\text{load}} = 50\ \Omega$.

For the evaluation, from Fig. 2(a), the dc biasing nodes V_{b1}, V_{b2}, and $V_{DD1} = V_{DD2}$ are biased separately through external voltage sources. Fig. 4 shows the measured S-parameters of the designed UWB amplifier. As can be seen in Fig. 4, the measured input return loss (S_{11}) is higher than 9.0 dB over a 3–5-GHz range. The output return loss (S_{22}) is higher than 11 dB for the same frequency range due to the source follower output stage. The maximum power gain (S_{21}) is $+9.8$ dB and the -3-dB bandwidth covers 2–4.6 GHz. In Fig. 4, the amplifier shows early power gain roll off near 4.6 GHz compared to the simulated value of 5 GHz. This is caused by the increase in value of the peaking inductance due to the addition of external bonding wires to the supply voltage, which had not been counted properly during the simulation. As can be seen from Fig. 4, the reverse isolation (S_{12}) approaches the 20-dB range due to the feedback network. Considering the reverse isolation provided by the source follower stage, the amount of reverse isolation is worse than expected. Fig. 5 shows both the measured and simulated NF of the implemented amplifier. The measured NF shows a minimum value of 2.3 dB at 3 GHz and stays at less than 3 dB up to 4 GHz, but rises up to 5.2 dB at 5 GHz. Compared to the simulation, the steep increase in NF near 5 GHz is caused by the lower power gain at these frequencies. The discrepancy in NF between the simulation and measurements at the 2–4-GHz range is the result of inaccuracies in the transistor noise model. From the simulation, the feedback resistor R_f degrades the amplifier NF to approximately 0.6 dB. The input referred IP3 is measured as -7 dBm for the two-tone signals of 4 GHz and 4.5 GHz. Fig. 6 shows the microphotograph of the fabricated CMOS UWB LNA with a chip size of 0.9 mm^2. Table I summarizes the measurement results and compares them with previously reported works. In Table I, the indicated amount of power dissipation for this work represents the power dissipated in the cascode topology only.

IV. Conclusion

A new CMOS UWB LNA, applied to the lower band (3.1–5 GHz) UWB system, is presented. The proposed ampli-

TABLE I
COMPARISON OF WIDEBAND CMOS LNA PERFORMANCES: PUBLISHED AND THE PRESENT WORKS

Ref.	$BW_{3\text{-}dB}$ (GHz)	S_{11} (dB)	Gain (dB)	NF* (dB)	IIP3 (dBm)	Power (mW)	Topology	Technology	Year
[3]	0.5 ~ 5.5	< -7	6.5	5.7	-	83.4	Distributed (single-ended)	0.6 μm CMOS	2000
[4]	0.6 ~ 22	< -8	8.1	4.3	-	52	Distributed (single-ended)	0.18 μm CMOS	2003
[5]	0.02 ~ 1.6	< -8	13.7	~1.9	0	35	Feedback (single-ended)	0.25 μm CMOS	2002
[6]	1 ~ 7	< -7.2	13.1	3.3	-4.7	75	Feedback (differential)	0.18 μm CMOS	2003
[8]	2.4 ~ 9.5	< -9.9	9.3	4	-6.7	9**	*LC*-filter based (single-ended)	0.18 μm CMOS	2004
[9]	2 ~ 10	< -10	21	2.5	-5.5	27**	*LC*-filter based (single-ended)	SiGe	2004
This work	**2 ~ 4.6**	**< -9**	**9.8**	**2.3**	**-7**	**12.6****	**Proposed (single-ended)**	**0.18 μm CMOS**	**2004**

* Minimum NF in pass band ** Only core LNA

fier topology adopts the conventional resistive shunt-feedback onto a narrowband LNA topology. In the proposed topology, the wideband characteristics are obtained by utilizing the feedback resistor as a component to reduce the Q-factor of the narrowband amplifier input impedance. The feedback resistor helps to extend the bandwidth of the amplifier as well as the gain flatness, while contributing a small amount in NF degradation. The adoption of the narrowband amplifier allows lower amounts of dc power dissipation. The proposed topology is applied for a 3.1–5-GHz UWB amplifier implementation based on 0.18-μm CMOS technology. The measured results shows more than 9 dB of input return loss, a higher than 11 dB output return loss, a peak gain of 9.8 dB over the -3-dB bandwidth of 2–4.6 GHz, while dissipating 7 mA from a 1.8-V supply. The minimum NF is 2.3 dB at 3 GHz and stays at less than 3 dB up to 4 GHz, but rises up to 5.2 dB at 5 GHz. The proposed LNA shows advantages in overall performance (NF, power gain, power dissipation, chip size, number of external components, etc.), compared to the distributed, conventional shunt-feedback, or filter-based amplifiers that make up other wideband topologies.

REFERENCES

[1] "Multi-band OFDM Physical Layer Proposal," IEEE P802.15 Working Group for Wireless Personal Area Networks (WPANs), http://grouper.ieee.org/groups/802/15/pub/2003/Jul03/03267r5P802_15_TG3a-Multi-band-OFDM-CFP-Presentation.ppt.

[2] "XtremeSpectrum CFP Presentation," IEEE P802.15 Working Group for Wireless Personal Area Networks (WPANs), http://grouper.ieee.org/groups/802/15/pub/2003/Jul03/03153r9P802-15_TG3a-XtremeSpectrum-CFP-Presentation.ppt.

[3] B. M. Ballweber, R. Gupta, and D. J. Allstot, "A fully integrated 0.5–5.5-GHz CMOS distributed amplifier," *IEEE Trans. Solid-State Circuits*, vol. 35, no. 2, pp. 231–239, Feb. 2000.

[4] R.-C. Liu, K.-L. Deng, and H. Wang, "A 0.6–22 GHz broadband CMOS distributed amplifier," in *Proc. IEEE Radio Frequency Integrated Circuits (RFIC) Symp.*, June 8–10, 2003, pp. 103–106.

[5] F. Bruccoleri, E. A. M. Klumperink, and B. Nauta, "Noise canceling in wideband CMOS LNA's," in *IEEE ISSCC Dig. Tech. Papers*, vol. 1, Feb. 2002, pp. 406–407.

[6] S. Andersson, C. Svensson, and O. Drugge, "Wideband LNA for a multistandard wireless receiver in 0.18 μm CMOS," in *Proc. ESSCIRC*, Sep. 2003, pp. 655–658.

[7] B. Razavi, *Design of Analog CMOS Integrated Circuits*. New York: McGraw-Hill, 2001.

[8] A. Bevilacqua and A. M. Niknejad, "An ultra-wideband CMOS LNA for 3.1 to 10.6 GHz wireless receiver," in *IEEE ISSCC Dig. Tech. Papers*, 2004, pp. 382–383.

[9] A. Ismail and A. Abidi, "A 3 to 10 GHz LNA using a wideband LC-ladder matching network," in *IEEE ISSCC Dig. Tech. Papers*, 2004, pp. 384–385.

[10] T.-K. Nguyen *et al.*, "CMOS low noise amplifier design optimization techniques," *IEEE Trans. Microwave Theory Tech.*, vol. 52, no. 5, pp. 1433–1442, May 2004.

[11] T. H. Lee, *The Design of CMOS Radio-Frequency Integrated Circuits*. Cambridge, U.K.: Cambridge Univ. Press, 1998.

[12] S. S. Mohan *et al.*, "Bandwidth extension in CMOS with optimized on-chip inductors," *IEEE J. Solid-State Circuits*, vol. 35, no. 3, pp. 346–355, Mar. 2000.